




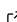


MotilA – A Python pipeline for the analysis of microglial fine process motility in 3D time-lapse multiphoton microscopy data

Fabrizio Musacchio¹ , Sophie Crux¹, Felix Nebeling¹, Nala Gockel¹, Falko Fuhrmann¹, and Martin Fuhrmann¹ 

¹ German Center for Neurodegenerative Diseases (DZNE), Bonn, Germany  Corresponding author

DOI: [10.xxxxxx/draft](https://doi.org/10.xxxxxx/draft)

Software

- [Review](#) 
- [Repository](#) 
- [Archive](#) 

Editor: [Open Journals](#) 

Reviewers:

- [@openjournals](#)

Submitted: 01 January 1970

Published: unpublished

License

Authors of papers retain copyright and release the work under a Creative Commons Attribution 4.0 International License ([CC BY 4.0](#)).

Summary

MotilA is an open-source Python pipeline for quantifying motility of microglial fine processes in 3D time-lapse two-channel fluorescence microscopy. It was developed for high-resolution *in vivo* multiphoton imaging and supports both single-stack and batch analyses. The workflow performs sub-volume extraction, optional registration and spectral unmixing, 2D z-projection, adaptive segmentation, and pixel-wise change detection across time to compute biologically interpretable metrics such as the fine-process turnover rate (TOR). The code is platform independent, documented with tutorials and an example dataset, and released under GPL-3.0.

Statement of need

Microglia are innate immune cells of the central nervous system and continuously remodel highly branched processes to survey brain tissue and to respond to pathology (M. Fuhrmann et al., 2010; Nimmerjahn et al., 2005; Prinz et al., 2019; Tremblay et al., 2010). Quantifying this subcellular motility is important for studies of neuroinflammation, neurodegeneration, and synaptic plasticity. Current practice in many labs relies on manual or semi-manual measurements in general-purpose tools such as Fiji/ImageJ or proprietary software (Carl Zeiss Microscopy GmbH, Accessed 2025; Schindelin et al., 2012). These procedures are time consuming, hard to reproduce, and poorly suited for cohort-level comparisons; they often analyze single cells rather than fields of view, and they are sensitive to user bias (Brown, 2017; Wall et al., 2018). There is no dedicated, open, and batch-capable solution tailored to this task.

MotilA fills this gap with an end-to-end, reproducible pipeline for 3D time-lapse two-channel imaging. It standardizes preprocessing, segmentation, and motility quantification and scales from individual stacks to large experimental cohorts. Although optimized for microglia, the approach generalizes to other motile structures that can be reliably segmented over time.

Implementation and core method

Input is a 5D stack in TZCYX or TZYX order, where T is time, Z is depth, C is channel, and YX are spatial dimensions. For each time point, *MotilA* extracts a user-defined z-sub-volume, optionally performs 3D motion correction and spectral unmixing, and computes a 2D maximum-intensity projection to enable fast and interpretable segmentation. After adaptive thresholding, the binarized projection at time t_i , denoted $B(t_i)$, is compared with $B(t_{i+1})$ to derive a temporal change map

$$\Delta B(t_i) = 2B(t_i) - B(t_{i+1}).$$

37 Pixels are classified as stable “S” ($\Delta B = 1$), gained “G” ($\Delta B = -1$), or lost “L” ($\Delta B = 2$).
38 From these counts, the turnover rate is defined as

$$TOR = \frac{G + L}{S + G + L},$$

39 representing the fraction of pixels that changed between consecutive frames. This pixel-based
40 strategy follows earlier microglial motility work (M. Fuhrmann et al., 2010; Nebeling et al.,
41 2023) while providing a fully automated and batchable implementation with parameter logging
42 and diagnostics.

43 The pipeline exposes options for 3D or 2D registration, contrast-limited adaptive histogram
44 equalization, histogram matching across time to mitigate bleaching, and median or Gaussian
45 filtering (Pizer et al., 1987; Virtanen et al., 2020; Walt et al., 2014). Results include segmented
46 images and overlays, per-time-point G, L, S, and TOR values, brightness and area traces,
47 and summary spreadsheets for downstream statistics. Memory-efficient reading and chunked
48 processing of large TIFFs are supported via Zarr (Miles et al., 2025).

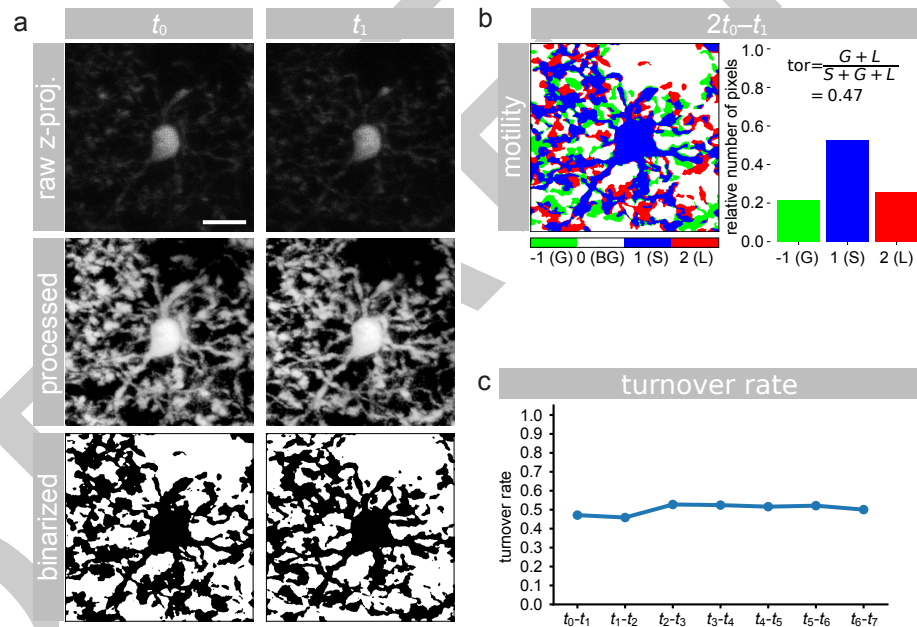


Figure 1: Example analysis with MotiA. **a)** z-projected microglial images at two consecutive time points (t_0 , t_1), shown as raw, processed, and binarized data. **b)** pixel-wise classification of gained (G), stable (S), and lost (L) pixels used to compute the turnover rate (TOR). **c)** TOR values across time points from the same dataset, illustrating dynamic remodeling of microglial fine processes. Scale bar represents 10 μm .

49 Usage

50 *MotiA* can be called from Python scripts or Jupyter notebooks. Three entry points cover
51 common scenarios: `process_stack` for a single stack, `batch_process_stacks` for a project
52 folder organized by dataset identifiers with a shared metadata sheet, and `batch_collect` to
53 aggregate metrics across datasets. All steps write intermediate outputs and logs to facilitate
54 validation and reproducibility. *MotiA*'s GitHub repository provides tutorials and an example
55 dataset to shorten onboarding.

Applications and scope

MotilA has been applied to quantify microglial process dynamics in several *in vivo* imaging studies and preprints (Crux et al., 2024; F. Fuhrmann et al., 2024; Gockel et al., 2025). Typical use cases include baseline surveillance behavior, responses to neuroinflammation or genetic perturbations, and deep three-photon imaging where manual analysis is impractical. The binarize-and-compare principle can in principle be adapted to other structures such as dendrites or axons when segmentation across time is robust.

Limitations

Using 2D projections simplifies processing but sacrifices axial specificity and can merge overlapping structures. Segmentation quality determines accuracy and can be affected by vessels, low signal-to-noise ratios, or strong intensity drift. The current spectral unmixing implementation is a simple subtraction, and more advanced approaches may be needed for some fluorophore combinations. *MotilA* targets pixel-level process motility rather than object-level tracking or full morphometry.

Example dataset

The repository includes two *in vivo* two-photon time-lapse stacks from mouse frontal cortex formatted for direct use with *MotilA* (Gockel et al., 2025). Each stack contains eight time points at five-minute intervals, two channels for microglia and neurons, and approximately sixty z-planes at one micrometer steps in a field of view of about 125 by 125 micrometers. The example reproduces the full analysis, including projections, segmentation, change maps, brightness traces, and TOR over time, and serves as a template for cohort-level workflows.

Availability

Source code, documentation, tutorials, and issue tracking are hosted at: <https://github.com/FabrizioMusacchio/motila>. The software runs on Windows, macOS, and Linux with Python 3.9 or newer and standard scientific Python stacks. It is released under GPL-3.0, and contributions via pull requests or issues are welcome.

Acknowledgements

We thank the Light Microscopy Facility and Animal Research Facility at the DZNE, Bonn, for essential support. This work was supported by the DZNE and grants to MF from the ERC (MicroSynCom 865618) and the DFG (SFB1089 C01, B06; SPP2395). MF is a member of the DFG Excellence Cluster ImmunoSensation2. Additional support came from the iBehave network and the CANTAR network funded by the Ministry of Culture and Science of North Rhine-Westphalia, and from the Mildred-Scheel School of Oncology Cologne-Bonn. Animal procedures for the example dataset followed institutional and national regulations, with efforts to reduce animal numbers and refine procedures.

References

- Brown, D. L. (2017). Bias in image analysis and its solution: Unbiased stereology. *Journal of Toxicologic Pathology*, 30(3), 183–191. <https://doi.org/10.1293/tox.2017-0013>
- Carl Zeiss Microscopy GmbH. (Accessed 2025). *ZEISS ZEN Microscopy Software*. <https://www.zeiss.com/metrology/en/software/zeiss-zen-core.html>.
- Crux, S., Roggan, M. D., Poll, S., Nebeling, F. C., Schiweck, J., Mittag, M., Musacchio, F., Steffen, J., Wolff, K. M., Baral, A., Witke, W., Gurniak, C., Bradke, F., & Fuhrmann, M. (2024). Deficiency of actin depolymerizing factors ADF/Cfl1 in microglia decreases motility and impairs memory. *bioRxiv*. <https://doi.org/10.1101/2024.09.27.615114>

- 100 Fuhrmann, F., Nebeling, F. C., Musacchio, F., Mittag, M., Poll, S., Müller, M., Giovannetti, E.
 101 A., Maibach, M., Schaffran, B., Burnside, E., Chan, I. C. W., Lagurin, A. S., Reichenbach,
 102 N., Kaushalya, S., Fried, H., Linden, S., Petzold, G. C., Tavano, S., Bradke, F., &
 103 Fuhrmann, M. (2024). Three-photon in vivo imaging of neurons and glia in the medial
 104 prefrontal cortex with sub-cellular resolution. *bioRxiv*. [https://doi.org/10.1101/2024.08.](https://doi.org/10.1101/2024.08.28.610026)
 105 [28.610026](https://doi.org/10.1101/2024.08.28.610026)
- 106 Fuhrmann, M., Bittner, T., Jung, C. K. E., Burgold, S., Page, R. M., Mitteregger, G., Haass,
 107 C., LaFerla, F. M., Kretschmar, H., & Herms, J. (2010). Microglial Cx3cr1 knockout
 108 prevents neuron loss in a mouse model of alzheimer's disease. *Nature Neuroscience*, 13(4),
 109 411–413. <https://doi.org/10.1038/nn.2511>
- 110 Gockel, N., Nieves-Rivera, N., Druart, M., Jaako, K., Fuhrmann, F., Rožkalne, R., Musacchio,
 111 F., Poll, S., Jansone, B., Fuhrmann, M., & Magueresse, C. L. (2025). *Example datasets for*
 112 *microglial motility analysis using the MotiA pipeline*. Zenodo. [https://doi.org/10.5281/](https://doi.org/10.5281/zenodo.15061566)
 113 [zenodo.15061566](https://doi.org/10.5281/zenodo.15061566)
- 114 Miles, A., jakirkham, Hamman, J., Orfanos, D. P., Stansby, D., Bussonnier, M., Moore,
 115 J., Bennett, D., Augspurger, T., Rzepka, N., Cherian, D., Verma, S., Bourbeau, J.,
 116 Fulton, A., Abernathy, R., Lee, G., Spitz, H., Kristensen, M. R. B., Jones, M., &
 117 Schut, V. (2025). *Zarr-developers/zarr-python: v3.0.6* (Version v3.0.6). Zenodo. <https://doi.org/10.5281/zenodo.3773449>
- 118
- 119 Nebeling, F. C., Poll, S., Justus, L. C., Steffen, J., Keppler, K., Mittag, M., & Fuhrmann,
 120 M. (2023). Microglial motility is modulated by neuronal activity and correlates with
 121 dendritic spine plasticity in the hippocampus of awake mice. *eLife*, 12, e83176. <https://doi.org/10.7554/eLife.83176>
- 122
- 123 Nimmerjahn, A., Kirchhoff, F., & Helmchen, F. (2005). Resting microglial cells are highly
 124 dynamic surveillants of brain parenchyma in vivo. *Science*, 308(5726), 1314–1318. <https://doi.org/10.1126/science.1110647>
- 125
- 126 Pizer, S. M., Amburn, E. P., Austin, J. D., Cromartie, R., Geselowitz, A., Greer, T., Haar
 127 Romeny, B. ter, Zimmerman, J. B., & Zuiderveld, K. (1987). Adaptive histogram equaliza-
 128 tion and its variations. *Computer Vision, Graphics, and Image Processing*, 39(3), 355–368.
 129 [https://doi.org/10.1016/S0734-189X\(87\)80186-X](https://doi.org/10.1016/S0734-189X(87)80186-X)
- 130 Prinz, M., Jung, S., & Priller, J. (2019). Microglia biology: One century of evolving concepts.
 131 *Cell*, 179(2), 292–311. <https://doi.org/10.1016/j.cell.2019.08.053>
- 132 Schindelin, J., Arganda-Carreras, I., Frise, E., Kaynig, V., Longair, M., Pietzsch, T., Preibisch,
 133 S., Rueden, C., Saalfeld, S., Schmid, B., & others. (2012). Fiji: An open-source platform
 134 for biological-image analysis. *Nature Methods*, 9(7), 676–682. [https://doi.org/10.1038/](https://doi.org/10.1038/nmeth.2019)
 135 [nmeth.2019](https://doi.org/10.1038/nmeth.2019)
- 136 Tremblay, M.-È., Lowery, R. L., & Majewska, A. K. (2010). Microglial interactions with
 137 synapses are modulated by visual experience. *PLOS Biology*, 8(11), 1–16. [https://doi.org/](https://doi.org/10.1371/journal.pbio.1000527)
 138 [10.1371/journal.pbio.1000527](https://doi.org/10.1371/journal.pbio.1000527)
- 139 Virtanen, P., Gommers, R., Oliphant, T. E., Haberland, M., Reddy, T., Cournapeau, D.,
 140 Burovski, E., Peterson, P., Weckesser, W., Bright, J., Walt, S. J. van der, Brett, M.,
 141 Wilson, J., Millman, K. J., Mayorov, N., Nelson, A. R. J., Jones, E., Kern, R., Larson, E., ...
 142 Contributors, S. 1.0. (2020). SciPy 1.0: Fundamental algorithms for scientific computing
 143 in python. *Nature Methods*, 17, 261–272. <https://doi.org/10.1038/s41592-019-0686-2>
- 144 Wall, E., Blaha, L. M., Paul, C. L., Cook, K., & Endert, A. (2018). Four perspectives on
 145 human bias in visual analytics. In G. Ellis (Ed.), *Cognitive biases in visualizations* (pp.
 146 29–42). Springer International Publishing. https://doi.org/10.1007/978-3-319-95831-6_3
- 147 Walt, S. van der, Schönberger, J. L., Nunez-Iglesias, J., Boulogne, F., Warner, J. D., Yager,
 148 N., Gouillart, E., Yu, T., & contributors, the scikit-image. (2014). Scikit-image: Image

DRAFT